# Orientation of LamB Signal Peptides in Bilayers: Influence of Lipid Probes on Peptide Binding and Interpretation of Fluorescence Quenching Data†

L. Voglino,‡ S. A. Simon,§ and T. J. McIntosh*,‡

*Departments of Cell Biology and Neurobiology, Duke University Medical Center, Durham, North Carolina 27710*

*Received January 15, 1999; Revised Manuscript Received April 7, 1999*

ABSTRACT: The orientation in lipid bilayers of the signal sequence of the bacterial protein LamB was studied using binding, circular dichroism, and fluorescence quenching experiments. Measurements were made of binding modifications caused by the incorporation of lipid probes (brominated or nitroxide-labeled phospholipids) used in the parallax fluorescence quenching method of determining peptide penetration depth [Abrams, F. S., and London, E. (1992) *Biochemistry 31*, 5312−5322]. The signal peptide bound to a similar extent to neutral bilayers composed of either egg phosphatidylcholine (EPC) or phosphatidylcholines brominated at various positions on their acyl chains. The fluorescence of a tryptophan in either the 18 or 24 position of the peptide was quenched more by bromines in the 6 and 7 than in the 9 and 10 positions on the lipid hydrocarbon chain. Parallax calculations showed that tryptophan-18 was located only 4 Å from the hydrocarbon−water interface, consistent with the peptide adopting a "hammock" configuration in the bilayer, with both termini exposed to the aqueous phase and the central α-helix located near the hydrocarbon−water interface. In contrast, the incorporation of 10% nitroxide-labeled lipids into EPC bilayers modified peptide binding in a manner dependent on the position of the nitroxide on the hydrocarbon chain; 7-Doxyl PC reduced the percent peptide bound by about one-half, whereas 12-Doxyl PC had little effect on binding. These binding differences modified tryptophan quenching by these probes, making parallax analysis problematical. In the presence of the positively charged LamB peptide, the incorporation of negatively charged phospholipids into EPC bilayers increased the level of peptide binding and modified tryptophan quenching by nitroxide probes. These results suggest that the nitroxide probe could be partially excluded from negatively charged lipid domains where the peptide preferentially bound. Quite different binding and quenching results were obtained with a negatively charged peptide analogue, showing that the charge on both the peptide and bilayer affects peptide−nitroxide probe interactions.

Knowledge of the location of peptides or proteins in lipid bilayers is critical to an understanding of peptide−lipid interactions and the function of membrane-bound peptides or proteins. Structural information about the location and orientation at atomic or near-atomic resolution has been obtained for only a limited number of membrane-bound proteins by X-ray crystallography (*1*−*4*) or electron microscopy (*5*−*8*). In part due to the lack of suitable crystals, there have been relatively few high-resolution X-ray or EM analyses of biologically relevant peptides in lipid bilayers. To obtain information about the location and orientation of peptides in bilayers, other methods have been used (*9*), including nuclear magnetic resonance (*10*, *11*), electron paramagnetic resonance (*12*, *13*), infrared spectroscopy (*14*−*17*), and fluorescence spectroscopy (*14*, *17*, *18*). In particular, the parallax method of interpreting fluorescence quenching data (*18*−*21*) has been used to obtain the depth in the bilayer hydrocarbon region of tryptophan or tyrosine residues of several types of peptides (*21*−*25*).

Peptides of particular interest have been the signal (leader) sequence of bacterial proteins, whose interaction with bilayers has been studied by a variety of techniques (*26*−*31*), including fluorescence quenching (*27*, *32*). Signal or leader sequences are N-terminal extensions on proteins that must pass through the plasma membrane. Both prokaryotic and eukaryotic signal sequences have a net positive charge on their N-termini, a central hydrophobic region, and a polar cleavage region (*33*, *34*). Although signal sequences interact with proteinaceous components of the export apparatus (*34*−*36*), there is evidence that during membrane translocation the signal sequence is in direct contact with lipids (*37*), suggesting a possible role for membrane lipids in the translocation process. Studies have shown that the hydrophobic regions of specific bacterial protein signal sequences form α-helices when associated with micelles or bilayers (*26*, *29*, *31*, *38*−*40*). In the case of the leader sequence of the bacterial protein LamB, it has also been shown that its level of binding to bilayers is strongly increased by the presence of negatively charged phospholipids in the bilayer, as expected from electrostatic attraction (*27*, *28*, *31*).

One controversial aspect of the LamB signal sequence interactions with bilayers is its location and orientation in the bilayer. When it is added to preformed lipid vesicles, there is agreement that the N-terminus of the peptide is localized near the outer surface of the bilayer (*27*, *31*, *32*,

† This work was supported by Grant GM-27278 from the National Institutes of Health.

‡ Department of Cell Biology.

§ Department of Neurobiology.

10.1021/bi990099q CCC: $18.00 
Published on Web 05/13/1999

*40*). However, various models have been presented for the location of the C-terminus of this 25-amino acid LamB peptide. Microelectrophoresis experiments with LamB peptides containing charged residue substitutions near the C- and N-termini indicated that both termini are located on the outside of the vesicle (*31*). These data were interpreted in terms of a "hammock" configuration for the peptide where both termini are anchored to the outside of the bilayer and the hydrophobic α-helix is located in the hydrocarbon region near the hydrocarbon−water interface (*31*). This hammock model is also consistent with tryptophan fluorescence experiments that showed much larger blue shifts (indicative of insertion into the bilayer hydrocarbon region) when the tryptophan was at position 18 (in the hydrophobic core of the peptide) than when it was at position 24 (near the C-terminus) (*27*, *32*). Different models of the peptide orientation in bilayers were obtained from parallax analysis of fluorescent quenching experiments with nitroxide-labeled lipids in vesicles composed of mixtures of zwitterionic phosphatidylethanolamine (PE) and negatively charged phosphatidylglycerol (PG) (*27*). It was calculated that the tryptophan residue placed at the 24 position of the peptide was located 8 Å into the acyl chain region of the bilayer, indicating a partial insertion of the C-terminal end of the peptide into the bilayer (*27*). This result is inconsistent with a hammock model. However, there are two potential problems with the interpretation of the results from the fluorescence quenching experiments using Doxyl-labeled lipids and LamB peptide. First, as noted by Abrams and London (*18*), to use the parallax method to calculate amino acid depth, fluorescence quenching must be measured in samples that have the same amount of bound fluorophore. Therefore, it is necessary to show that the presence of the probe lipid does not alter peptide binding. In this regard, Voglino et al. (*31*) found that the percent of LamB peptide bound to bilayers composed entirely of 7-Doxyl PC was less than 1%, compared to more than 40% bound to EPC bilayers. Second, as noted by Jones and Gierasch (*27*), the local concentration of the Doxyl-labeled PC lipid may not reflect its bulk concentration in the bilayer. This may be important in experiments with the positively charged LamB peptide and vesicles containing mixtures of zwitterionic and charged phospholipids, because some positively charged peptides or proteins cause clustering or partial phase separation of the negatively charged lipids (*41*−*43*). Such a variation in the local distribution of the lipid probes could affect the interpretation of the quenching experiments (*44*).

In this paper, we pursue the question of the orientation and location of the LamB signal peptide in phospholipid bilayers by using binding, circular dichroism, and fluorescence data to assess whether (1) the relatively small concentration (10 mol %) of nitroxide lipids usually used in fluorescent quenching experiments affects the binding of the LamB peptide, (2) the position of the nitroxide group on the lipid hydrocarbon chain affects peptide binding, (3) different fluorescent quenchers, namely, brominated lipids, modify LamB peptide binding, and (4) the net charge on the LamB peptide can affect peptide−probe interactions. Finally, we use these data to test the hammock (*31*) and partial lipid penetration models (*27*) for the LamB orientation in the bilayer.

Table 1: Peptide Sequences[a]

| | |
|---|---|
| LamB | $NH_3^+$·MMITLR$^+$K$^+$LPLAVAVAAGVMSAQAMA·$COO^-$ |
| LamB-18W | $NH_3^+$·MMITLR$^+$K$^+$LPLAVAVAAGWMSAQAMA·$COO^-$ |
| LamB-24W | $NH_3^+$·MMITLR$^+$K$^+$LPLAVAVAAGVMSAQAWA·$COO^-$ |
| LamB-EE | $NH_3^+$·MMITLE$^-$E$^-$LPLAVAVAAGWMSAQAMA·$COO^-$ |

[a] Amino acid substitutions are underlined, and charges are indicated for each sequence.

## MATERIALS AND METHODS

*Materials.* Egg phosphatidylcholine (EPC), brain phosphatidylserine (PS) (sodium salt), 1-palmitoyl-2-oleoyl-*sn*-3-[phospho-*rac*-(1-glycerol)] (POPG), the nitroxide spin probes 1-palmitoyl-2-stearoyl (7-Doxyl)-*sn*-glycerol-3-phosphocholine (7-Doxyl PC), 1-palmitoyl-2-stearoyl (12-Doxyl)-*sn*-glycerol-3-phosphocholine (12-Doxyl PC), the brominated phospholipids 1-palmitoyl-2-stearoyl (6,7-dibromo)-*sn*-glycero-3-phosphocholine (6,7-Br PC), 1-palmitoyl-2-stearoyl (9,-10-dibromo)-*sn*-glycero-3-phosphocholine (9,10-Br PC), and 1-palmitoyl-2-stearoyl (11,12-dibromo)-*sn*-glycero-3-phosphocholine (11,12-Br PC), and the fluorescently labeled phosphatidylserine NBD-PS were all purchased from Avanti Polar Lipids (Alabaster, AL). All chemicals were used without further purification. Buffers were made using Hepes (sodium salt) and doubly distilled water. Unless otherwise noted, our standard buffer was 2 mM Hepes adjusted to pH 7.4 with NaOH.

*Peptide Synthesis and Purification.* Peptides were synthesized by the Micro Protein Chemistry Facility at the University of North Carolina (Chapel Hill, NC) using FMOC chemistry in a Symphony (Rainin) peptide synthesizer. The peptides were purified by HPLC and analyzed by time-of-flight MALDI III (Shimadzu/Kratos) mass spectrometry. Analogues to the signal sequence peptide of *Escherichia coli* LamB were synthesized with a tryptophan substituted for the valine at position 18 (LamB-18W) or 24 (LamB-24W) (Table 1). At pH 7.4, both of these peptides have three positive charges near their N-termini. Another analogue (LamB-EE) was synthesized with the tryptophan substitution at position 18, but with negatively charged glutamic acids (E) substituted for the positively charged residues at positions 6 and 7. Thus, at pH 7.4, both LamB-18W and LamB-24W had a net charge of +2, whereas LamB-EE had a net charge of −2 (Table 1).

*Preparation of Liposomes.* Multilamellar liposomes (MLVs) were made by standard methods (*45*) as described previously (*31*). The appropriate lipids were codissolved in chloroform/methanol (2:1 v:v) which was subsequently removed by rotary evaporation. The lipids were hydrated in 2 mM Hepes buffer and extensively vortexed.

Small unilamellar vesicles (SUVs) were prepared by probe sonication of MLVs (*45*). Briefly, MLVs were sonicated at 40 W with a Disruptor Excell 2005 sonifier cell (Heat Systems) with a 19 mm flat tip under a continuous $N_2$ flow for five cycles consisting of 2 min in the sonication mode and 2 min in the standby mode. Before use, the SUV suspensions were centrifuged at 100000*g* for 10 min to sediment metal particles, undispersed lipid, and MLVs. Lipid concentrations were determined by inorganic phosphorus measurements (*46*). SUVs, rather than large unilamellar vesicles (LUVs), were used in the circular dichroism and fluorescence experiments to reduce light scattering. Previous

experiments have shown that the binding of LamB-18W is similar to SUVs and LUVs (*31*).

*Circular Dichroism (CD).* CD measurements were taken on an Aviv 62DS spectropolarimeter equipped with a CoolFlow CFT-33 (Neslab) temperature controller. CD spectra of the peptides were obtained at 25 °C using a 1 mm path length quartz cuvette, a 0.5 nm step size, and a 1 s per step acquisition time. Spectra were averaged over 20 scans. For peptides in buffer, spectra were recorded from 185 to 260 nm. For experiments with neutral bilayers, in which the extent of peptide binding is relatively small (*28*, *31*) and thus gives a lower signal-to-noise ratio, peptide−lipid spectra were obtained from 200 to 260 nm. All spectra were baseline-corrected. In the peptide−lipid samples, a background CD spectrum was recorded from the buffer with the same lipid concentration used in the sample. To avoid possible problems with peptide aggregation (*26*), we used 5 $\mu$M peptide. The lipid concentration was varied from 0 to 4 mM. Higher lipid concentrations were not used due to problems with light scattering. Each lipid−peptide sample was prepared independently, rather than by serial dilution. Ellipticity measurements at 222 nm, reported as mean molar residue ellipticity ($\vartheta_{222}$ in deg cm$^2$ dmol$^{-1}$), were measured over an average of 60 points. Standard deviations were less than 10%.

*Fluorescence Measurements.* Fluorescence emission spectra of the peptide's tryptophan were measured with quartz cuvettes (1.0 or 0.25 cm) over the range of 320−400 nm using an excitation wavelength of 280 nm with a Fluoromax DM3000 (Spex Industries, Edison, NJ) photon counting fluorometer operating in the signal/reference mode and equipped with a water bath circulator for maintaining the temperature at 25 °C. Spectra were collected with a step size of 0.5 nm with an averaging time of 4 s/nm. Where appropriate, measurements were corrected for blank suspensions of buffer or lipid in buffer. Blue shifts were calculated as the difference in wavelength of the maxima in emission spectra of lipid−peptide and peptide samples. Standard deviations in the blue shift were less than 0.5 nm.

Quenching measurements were performed with an excitation wavelength of 280 nm and an emission wavelength of 340 nm for LamB-18W or LamB-24W with EPC or 65:35 EPC/POPG in the presence and absence of 10 mol % Doxyl PCs and also with brominated PCs. Each experiment was repeated at least three times. The values of the fluorescence intensity in the absence ($I_o$) and presence ($I$) of quencher were measured at 340 nm. Parallax analysis was performed according to published procedures (*18*, *19*, *21*). Specifically, the distance of the tryptophan residue from the bilayer center ($Z_{CF}$) is given by

$$Z_{CF} = L_{C1} + [-\ln(F_1/F_2)/\pi C - L_{21}^2]/2L_{21} \qquad (1)$$

where $L_{C1}$ represents the distance from the bilayer center to the shallow quencher which is 10.8 Å for 6,7-Br PC (*47*), $C$ is the mole fraction of quencher (1 for brominated lipids) divided by the lipid area (70 Å$^2$), $F_1$ and $F_2$ are the relative fluorescence intensities of the shallower and deeper quenchers, respectively, and $L_{21}$ is the difference in the depth of the two quenchers. We use 0.9 Å per $CH_2$ or $CBr_2$ group (*47*). The probe insertion depth is equal to one-half the bilayer thickness minus $Z_{CF}$, where for these brominated lipids the bilayer thickness is equal to 29 Å (*47*).

*Binding Measurements.* As described previously (*31*), the extent of binding of peptides to lipid vesicles was measured with an ultrafiltration assay (*48*) that separated lipid and lipid−peptide complexes from free peptide with Centrifree (Amicon) filters. In all binding studies, the peptide concentration was 5 $\mu$M and the phospholipid concentration was 1.5 mM. This phospholipid concentration was chosen to ensure that the filters did not become clogged. For the binding assay, peptide−SUV samples were incubated for 10 min, and then divided into six aliquots which were centrifuged for 15 min at 1000*g* through the Amicon filters. Peptide recovery in the absence of lipid was greater than 95%, and phosphate analysis (*46*) revealed that no lipid was in the eluate. The free peptide concentration was measured in each eluate by tryptophan fluorescence at 352 nm. The standard deviation for the six readings was always less than 10%. The amount of peptide bound to the lipid was determined by subtracting the free peptide concentration from the total peptide concentration.

Partition coefficients were calculated from the binding measurements according to the procedure described previously (*31*). Under conditions where the concentration of peptide in the bilayer is much smaller than the molar concentration of lipid, one may write for the mole fraction partition coefficient

$$K_p = (P_{bil}W)/(P_{wat}L) \qquad (2)$$

where $P_{bil}$ and $P_{wat}$ are the bulk concentrations of peptide in the bilayer and water, respectively, and $L$ and $W$ are the molar concentrations of lipid and water, respectively (*49*). For SUVs, $L$ was taken to be 66% of the total lipid concentration with the assumption that the peptide bound only to the outer monolayer of the bilayer (*31*). The free energies of transfer of the peptide from the buffer to the bilayer were calculated from $\Delta G = -RT \ln K_p$.

## RESULTS

Circular dichroism, fluorescence blue shift experiments, and direct binding measurements were used to investigate the association of LamB-18W with bilayers composed of EPC, 6,7-Br PC, 7-Doxyl PC, and a 9:1 mixture of EPC and 7-Doxyl PC. The binding experiments (Figure 1A and Table 2) showed that the percentage of LamB-18W bound was similar for EPC (43.7 ± 3.1%) and 6,7-Br PC (37.1 ± 3.0%), but was markedly lower for 9:1 EPC/7-Doxyl PC (20.8 ± 0.3%). Previously, we (*31*) had shown that LamB-18W had a very low percent binding (0.8 ± 1.0%) to bilayers composed entirely of 7-Doxyl PC (also shown in Figure 1A). The free energies of transfer from the buffer to bilayer ($\Delta G$) are shown in Table 2. Here it is seen that the small differences in free energy between EPC and 9:1 EPC/7-Doxyl PC resulted in relatively large decreases in the percentage of peptide bound. For these lipid systems, the magnitude of the molar ellipticity at 222 nm ($\vartheta_{222}$) increased with increasing lipid concentration (Figure 1B), meaning that the amount of α-helix increased with lipid concentration (*31*). At the higher lipid concentration, the changes in $\vartheta_{222}$ were similar for EPC and 6,7-Br PC, were reduced for 9:1 EPC/7-Doxyl PC, and were much smaller for bilayers of 7-Doxyl PC

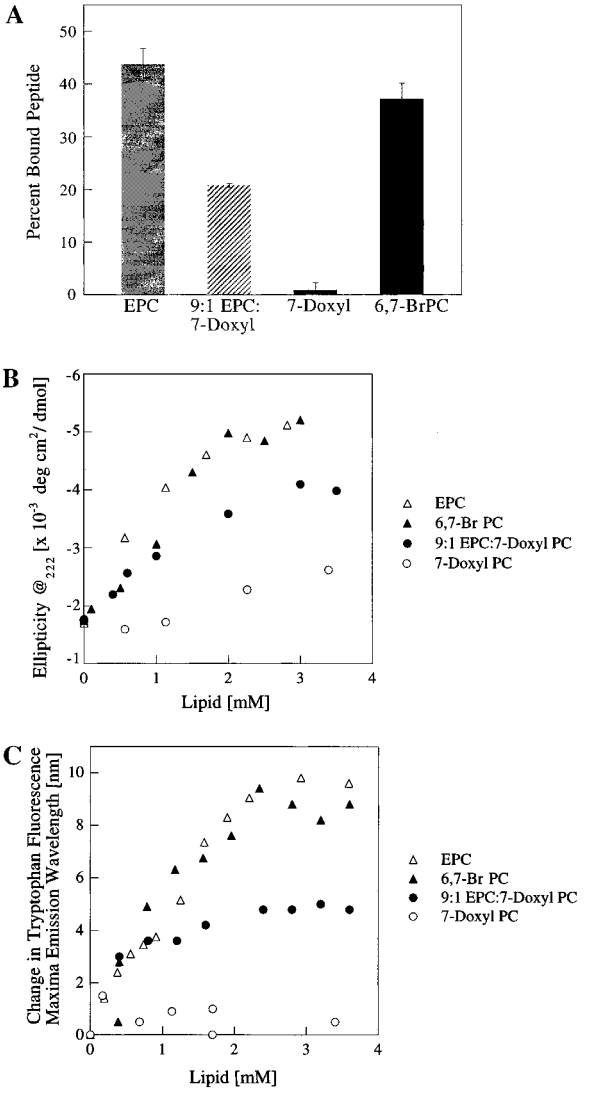


FIGURE 1: Association of LamB-18W (5 $\mu$M) with vesicles composed of EPC, 7-Doxyl PC, 9:1 EPC/7-Doxyl PC, and 6,7-Br PC. (A) Percentage of the peptide bound to vesicles at a lipid concentration of 1.5 mM. (B) Ellipticity at 222 nm ($\vartheta_{222}$) and (C) maximal change in tryptophan fluorescence maxima emission wavelength (blue shift) plotted as a function of EPC concentration.

Table 2: Binding Parameters

| lipid | % LamB-18W bound | $K_p$ | $\Delta G$ (kcal/mol) |
|---|---|---|---|
| EPC | 43.7 ± 3.1 | $4.28 \times 10^4$ | −6.2 |
| 9:1 EPC/7-Doxyl PC | 20.8 ± 0.3 | $1.45 \times 10^4$ | −5.6 |
| 9:1 EPC/12-Doxyl PC | 37.6 ± 3.6 | $3.33 \times 10^4$ | −6.1 |
| 6,7-Br PC | 37.1 ± 3.0 | $3.26 \times 10^4$ | −6.1 |
| 9,10-Br PC | 44.1 ± 1.9 | $4.35 \times 10^4$ | −6.2 |
| 11,12-Br PC | 38.2 ± 5.9 | $3.41 \times 10^4$ | −6.1 |
| EPC/POPG | 94.0 ± 5.1 | $8.65 \times 10^5$ | −8.0 |
| EPC/POPG/7-Doxyl PC | 93.9 ± 4.8 | $8.50 \times 10^5$ | −8.0 |
| EPC/POPG/12-Doxyl PC | 90.9 ± 3.2 | $5.51 \times 10^5$ | −7.7 |

(Figure 1B). Likewise, the changes in wavelength of the maximum in tryptophan fluorescence (blue shift) were similar for LamB-18W in EPC and 6,7-Br PC, reduced for 9:1 EPC/7-Doxyl PC, and much smaller for 7-Doxyl PC (Figure 1C).

Figure 2 and Table 2 compare the binding of LamB-18W to EPC and EPC bilayers containing 10 mol % 7-Doxyl PC and 10 mol % 12-Doxyl PC, and also to brominated PCs with the bromines at different positions along the chains (6,7-Br PC, 9,10-Br PC, and 11,12-Br PC). The data indicate that the percentage of bound LamB-18W was about the same for EPC and all three brominated lipids, independent of the presence and location of the bromines along the acyl chain. In contrast, for the nitroxide-labeled lipids, the binding depended on the location of the Doxyl group along the hydrocarbon chain, with binding being essentially unchanged by the presence of 10% 12 Doxyl PC but reduced by about 50% by the presence of 10 mol % 7-Doxyl PC (Table 2).

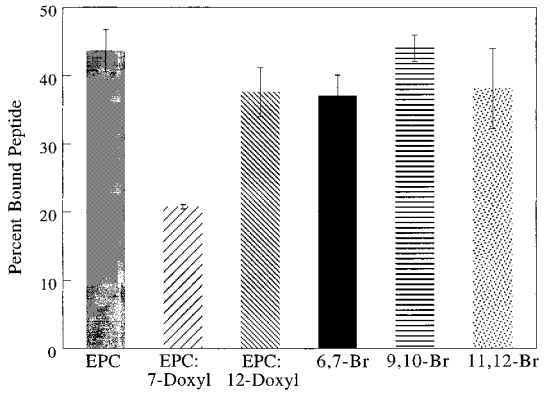


FIGURE 2: Binding of LamB-18W (5 $\mu$M) with vesicles (at a lipid concentration of 1.5 mM) composed of EPC, 9:1 EPC/7-Doxyl PC, 9:1 EPC/12-Doxyl PC, 6,7-Br PC, 9,10-Br PC, and 11,12-Br PC.

We also compared the binding of LamB-18W and LamB-24W to PC vesicles. The percentage of LamB-24W bound to EPC and the brominated PC bilayers was similar, being 39.0 ± 4.8, 41.8 ± 3.0, and 40.3 ± 2.5% for EPC, 6,7-Br PC, and 9,10-Br PC bilayers, respectively. These values were similar to those found for the percentage of LamB-18W bound to vesicles with the same compositions (Table 2). In addition, as was the case for LamB-18W (Table 2), the level of binding of LamB-24W was reduced (to 21.8 ± 3.8%) by the presence of 10 mol % 7-Doxyl PC in EPC bilayers.

Panels A and B of Figure 3 show fluorescence emission spectra for LamB-18W and LamB-24W in vesicles composed of EPC, 6,7-Br PC, and 9,10-Br PC. For LamB-18W (Figure 3A), the tryptophan fluorescence was quenched to a much greater extent by 6,7-Br PC than by 9,10-Br PC. For LamB-24W (Figure 3B), the tryptophan fluorescence was quenched by 6,7-Br PC, but was unquenched by 9,10-Br PC. Table 3 shows the values of $I_o/I$ for these data, where $I_o$ is the fluorescence intensity (measured at 340 nm) for EPC and $I$ is the fluorescence intensity for the brominated PCs. For these brominated lipids where the probe molecule did not affect the binding (Figure 2), we used the parallax method (eq 1) to calculate the location in the bilayer of the tryptophan at position 18. We found that this tryptophan was located in the hydrocarbon region at a $Z_{CF}$ of 10.7 Å, or at a penetration depth of about 3.8 Å from the hydrocarbon−water interface.

Quenching values for LamB-18W and LamB-24W in 9:1 EPC/7-Doxyl PC and 9:1 EPC/12-Doxyl PC are also shown in Table 3. For LamB-18W, the value of $I_o/I$ was larger for 9:1 EPC/12-Doxyl PC than for 9:1 EPC/7-Doxyl PC, whereas for LamB-24W, the value of $I_o/I$ was smaller for 9:1 EPC/12-Doxyl PC than for 9:1 EPC/7-Doxyl PC.

Binding and quenching experiments were also performed with the positively charged LamB-18W (+2) and the negatively charged LamB-EE (−2) (Table 1) in the presence of bilayers containing mixtures of zwitterionic and negatively

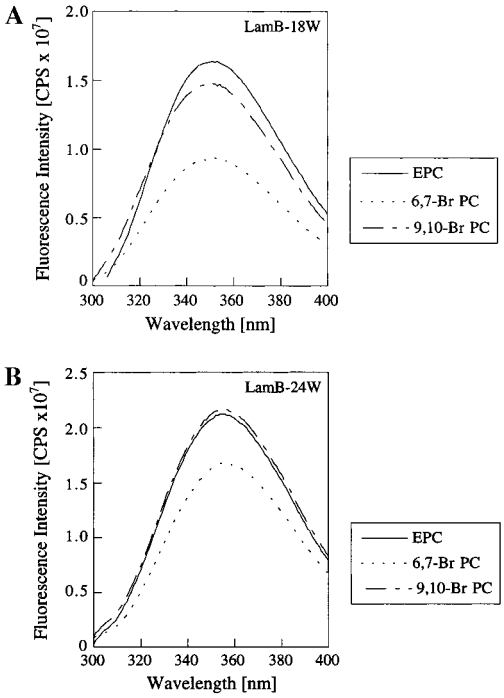


FIGURE 3: Fluorescence spectra for (A) LamB-18W and (B) LamB-24W with vesicles of EPC, 6,7-Br PC, and 9,10-Br PC. Peptide (5 $\mu$M) was used with SUVs at a lipid concentration of 1.5 mM.

Table 3: Fluorescence Quenching Data ($I_o/I$)

| | peptide | | |
|---|---|---|---|
| lipid | LamB-18W | LamB-24W | LamB-EE |
| 6,7-Br PC | 1.56 ± 0.02 | 1.27 ± 0.04 | − |
| 9,10-Br PC | 1.14 ± 0.04 | 1.03 ± 0.04 | − |
| EPC/7-Doxyl PC | 1.25 ± 0.06 | 1.29 ± 0.03 | − |
| EPC/12-Doxyl PC | 1.40 ± 0.04 | 1.14 ± 0.14 | − |
| EPC/POPG/7-Doxyl PC | 1.32 ± 0.04 | 1.14 ± 0.02 | 1.42 ± 0.06 |
| EPC/POPG/12-Doxyl PC | 1.16 ± 0.05 | 1.03 ± 0.02 | 1.56 ± 0.09 |

charged lipids (65:35 EPC/POPG). Figure 4A shows that the addition of the negatively charged POPG to EPC increased the percentage binding of LamB-18W from 43.7 ± 3.1 to 94.0 ± 5.1%. For these negatively charged bilayers, the presence of either 10 mol % 7-Doxyl PC or 12-Doxyl PC had no appreciable effect on binding (Figure 4A). However, as shown in Figure 4B, for these EPC/POPG bilayers the presence of 10 mol % 7-Doxyl decreased the level of binding of LamB-EE, whereas the presence of 10 mol % 12-Doxyl PC had a much smaller effect on the level of binding.

The fluorescence quenching results for LamB-18W, LamB-24W, and LamB-EE peptides and negatively charged bilayers containing Doxyl lipids are shown in Table 3. In the case of both LamB-18W and LamB-24W, the values of $I_o/I$ (compared to EPC/POPG) were larger for EPC/POPG/7-Doxyl PC than for EPC/POPG/12-Doxyl PC. However, for LamB-EE the value of $I_o/I$ was larger ($P = 0.13$ with the $t$ test) for EPC/POPG/7-Doxyl PC than for EPC/POPG/12-Doxyl PC bilayers.

Comparisons of the binding (Figures 2 and 4A,B and Table 2) and quenching data (Table 3) show the following correlations. Where the binding of the peptide was not appreciably affected by the presence of the quencher, such as the cases of LamB-18W to 6,7-Br PC and 9,10-Br PC (Figure 2) or LamB-18W to EPC/POPG in the presence and

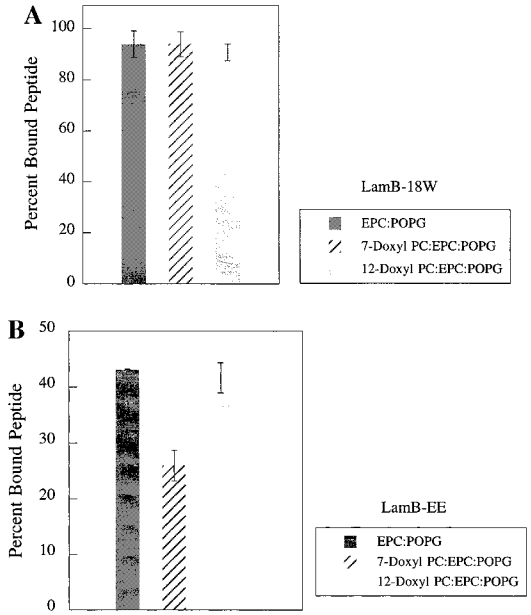


FIGURE 4: Binding of 5 $\mu$M (A) LamB-18W or (B) LamB-EE to vesicles (at a lipid concentration of 1.5 mM) composed of 65:35 EPC/POPG containing no nitroxide probe or 10 mol % 7-Doxyl PC or 12-Doxyl PC.

absence of nitroxide probes (Figure 4A), there were higher values of $I_o/I$ when the probe (either bromine atoms or the Doxyls) was closer to the lipid headgroup. However, in cases where the binding was affected by the presence and position of the probe, such as in the cases of the binding of LamB-18W to EPC/7-Doxyl PC and EPC/12-Doxyl PC (Figure 2) or LamB-EE binding to EPC/POPG/7-Doxyl PC and EPC/POPG/12-Doxyl PC (Figure 4B), there were larger values of $I_o/I$ when the Doxyl group was located at the 12 position on the hydrocarbon chain.

## DISCUSSION

The results of our CD, fluorescence, and binding experiments provide information about (1) the effects of specific lipid probes on the binding of LamB signal peptides to bilayers, (2) the conformation of the peptide in bilayers, and (3) effects of peptide charge on fluorescence quenching.

*Lipid Probes and Peptide Binding.* The data in Table 2 and Figures 1, 2, and 4 show that the presence in the bilayer of specific lipid probes can alter LamB peptide binding to the lipid membrane. The extent of this effect depends on the type of probe, the position of the probe in the lipid hydrocarbon chains, and the net charge on both the peptide and bilayer. That is, although all three of the brominated lipid probes tested did not effect LamB-18W or LamB-24W binding, in EPC bilayers nitroxide spin probes with the Doxyl located in the acyl chain near the lipid headgroup (7-Doxyl PC) markedly decreased the extent of binding whereas those with the nitroxide group further down the chain (12-Doxyl PC) had no appreciable effect on binding (Figures 1A and 2). Circular dichroism (Figure 1B) and blue shift (Figure 1C) results were consistent with these binding studies. Previously, we (*31*) had found that there was very little binding of LamB-18W to bilayers composed entirely of 7-Doxyl PC (panels A−C of Figure 1). Our new data show that the presence of the small amount (10 mol %) of this probe typically used in fluorescent quenching experiments

reduced the extent of binding of the LamB-18W peptide by about one-half. Comparisons of the free energies of binding of LamB-18W to EPC and 9:1 EPC/7-Doxyl PC (Table 2) indicate that relatively small changes in $\Delta G$ (0.6 kcal/mol $\approx K_BT$) can lead to these relatively large differences in the amount of bound peptide.

In the case of negatively charged EPC/POPG bilayers, the presence of 7-Doxyl PC had no effect on the binding of LamB-18W (Figure 4A), but significantly decreased the extent of binding of negatively charged LamB-EE (Figure 4B). We also note that LamB-EE bound to negatively charged EPC/POPG vesicles to a similar extent as LamB-18W bound to neutral EPC bilayers (Table 2) even though it might be expected that electrostatic repulsion would decrease the extent of binding of LamB-EE. As noted previously (*31*), a possible explanation is that the presence of PG would lower the pH near the bilayer surface (*50*) and the glutamic acids of LamB-EE might be closer to their p$K_a$'s and therefore not fully charged. To show that this may occur, we calculate the pH at the surface ($pH_s$) of a PC/PG (65:35) bilayer in 2 mM Hepes buffer (sodium salt) at pH 7.4. Under these conditions, the buffer has an ionic strength of about 0.002 M and the initial charge density ($\sigma_{init}$) of the bilayer (assuming an area per molecule of 70 $A^2$ for both PC and PG) is 35 $e^-$/7000 $Å^2$. The surface charge density, correcting for sodium binding to PG ($K \approx 1\ M^{-1}$), together with the linearized Gouy−Chapman equation (*51*) can be used to calculate the surface potential ($\Psi$). Thus, $C^{1/2} \times \sin h(zF\Psi/2RT) = 136\sigma_{init}/[1 + KC \times \exp(-zF\Psi/RT)]$, where $\Psi$ is the surface potential in millivolts, $z = 1$, $C = 0.002$ M, and $RT/F = 25.7$ mV at 298 K. Solving the equation for $\Psi$, we find that $\Psi$ equals −147 mV. Since counterions must screen the surface charge to preserve charge neutrality, the hydrogen ion concentration at the surface can be written as $[H^+]_s = [H^+]_{bulk} \exp(-\Psi/25.7\ mV)$ so that the pH at the bilayer surface is $pH_s = pH_{bulk} - \Psi/(2.3 \times 25.7) = 7.4 - 2.5 = 4.9$. Since the p$K_a$ of the side chain carboxyl group in glutamic acid is 4.25, under these low-ionic strength conditions LamB-EE should be significantly less charged at the bilayer surface, and hence, the effect of electrostatic repulsion should be reduced.

*Conformation of the LamB Signal Sequence in Bilayers.* In the cases where the binding data showed that the presence of the lipid probe did *not* modify peptide binding (Table 2), the fluorescence quenching data (Table 3) showed that the peptide tryptophans in both positions 18 and 24 were quenched more by probes located near the lipid headgroup than by probes located further down the acyl chain. That is, in the case of the brominated lipids for both LamB-18W and LamB-24W, $I_o/I$ was greater in 6,7-Br PC bilayers than in 9,10-Br PC bilayers (Table 3). Parallax analysis of these data indicates that the tryptophan at position 18 of the peptide (Table 1) was located 3.8 Å from the hydrocarbon−water interface. Although the parallax method could not be used for LamB-24W (because no significant quenching was seen for 9,10-Br PC), the data indicate that the tryptophan at position 24 was in a region with a low dielectric constant very near the lipid headgroup region. Similarly, for EPC/POPG bilayers for both LamB-18W and LamB-24W, $I_o/I$ was greater in bilayers containing 7-Doxyl PC than in bilayers containing 12-Doxyl PC (Table 3). These data imply that both the 18 and 24 positions of the peptide are located near the interfacial region of the bilayer, consistent with a hammock model for the peptide in the bilayer where both polar termini are exposed to the aqueous phase with the core of the nonpolar α-helix located in the hydrocarbon region of the bilayer near the hydrocarbon−water interface (*31*).

In the cases where the lipid Doxyl probe altered binding (LamB-18W with EPC and LamB-EE with EPC/POPG), the quenching data were quite different. That is, for these cases the values for $I_o/I$ were larger for bilayers containing 12-Doxyl PC than for bilayers containing 7-Doxyl PC. Taken by themselves, these particular quenching data could be interpreted to indicate that the tryptophan at position 18 was located closer to the 12-Doxyl in the bilayer than to the 7-Doxyl. However, that conclusion would only be valid if the binding data were similar for bilayers containing 7-Doxyl PC and 12-Doxyl PC (*18*), which was not the case for these LamB peptides in the range of lipid concentrations that we were using (Figures 2 and 4B). That is, for these lipid systems, the larger tryptophan fluorescence quenching by the 12-Doxyl than by the 7-Doxyl probe was probably due to the fact that there was more LamB-18W in the bilayer for EPC containing 12-Doxyl PC than for EPC containing 7-Doxyl PC (Figure 2) and there was more LamB-EE in the EPC/POPG bilayers containing 12-Doxyl PC than for those containing 7-Doxyl PC (Figure 4B). A higher degree of fluorescent quenching will occur when a higher percentage of peptide is located within the bilayer.

Thus, the parallax method, when applied to quenching data with brominated lipids (Table 3), clearly shows that the entire LamB peptide is located close to the hydrocarbon−water interface. However, with the nitroxide lipid probes our fluorescence quenching data cannot be readily interpreted with the parallax method because of the difference in binding for bilayers containing 7-Doxyl PC and 12-Doxyl PC (Figure 2). We raise the possibility that for LamB peptide the parallax results with nitroxide probes may be misleading because of the effects of the Doxyl lipid probes on peptide binding or lipid clustering in mixed phospholipid bilayers (see below). All of the other data, including the quenching results with brominated lipids (Table 3), blue shift results (*27*), and microelectrophoresis data (*31*), are consistent with the hammock model for the peptide topography in the bilayer.

The proposed hammock model of LamB binding can help explain, at least qualitatively, why 7-Doxyl PC modified the peptide binding to the bilayer. We (*31*) argued that the presence of the dipolar Doxyl group at position 7 on the acyl chain increases the effective width of the hydrophilic interfacial region of the bilayer, which in PC bilayers is approximately equal to the diameter of a peptide α-helix (*52*). With a hammock configuration, the hydrophobic α-helix would penetrate a limited distance into the bilayer hydrocarbon region. Therefore, if the 7-Doxyl PC increased the effective width of the hydrophilic region of the bilayer, it would prevent some of the hydrophobic amino acids in the peptide helix from reaching the low-dielectric region of the bilayer, thereby diminishing the hydrophobic free energy (Table 2). The hydrophobic effect is the major factor in driving LamB binding to electrically neutral bilayers (*31*). At present, it is not quantitatively understood why only 10 mol % 7-Doxyl PC reduced the extent of binding by as much as 50%. In the case of the brominated lipid probes, peptide binding was not affected by the probe, undoubtedly due to

the relatively small size and small dipole moment of the substituted bromines on the acyl chains.

*Effect of Charge on the LamB Signal Peptide.* The fluorescence quenching data were markedly different for LamB-18W and LamB-EE, indicating that the net charge on the peptide can affect peptide−probe interactions. One likely possibility for explaining these data is the sequestration of negatively charged lipids, and thus the depletion of Doxyl PC, in the region where the positively charged LamB-18W bound to the bilayer. Under such a circumstance, the concentration of probe molecules near the peptide could be different than that in the bulk of the bilayer which could effect quenching (*44*). Similar partial lipid phase separation in the plane of the bilayer has also been observed with other positively charged peptides (*41*, *42*). Domain formation arises when the free energy gain of neutralizing the electric double layer is greater than the free energy loss arising from the reduction in entropy that accompanies phase separation (*43*). The preferential binding of the LamB-18W to negatively charged domains can help explain why the Doxyl PC probes did not modify the binding of LamB-18W to the bilayer. This can be rationalized by the Doxyl PC being partially excluded from the predominantly negatively charged lipid domains where the peptide preferentially bound.

In the case of the negatively charged LamB-EE, there would be no sequestration of negatively charged lipids so that the nitroxide probes would be located in the region of peptide binding. Therefore, we argue that in EPC/POPG bilayers the binding of LamB-EE was modified by the presence of 7-Doxyl PC (Figure 4B) by a mechanism similar to that by which the binding of LamB-W was modified by 7-Doxyl PC in EPC bilayers (see above).

*Summary.* We have presented evidence for LamB signal peptide which shows that (1) the peptide assumes a hammock configuration in lipid bilayers, (2) nitroxide lipid probes, but not brominated lipids, affect the peptide binding to bilayers, and (3) the net charge on the peptide affects fluorescence quenching due to the formation of lipid microdomains. It remains to be determined whether these nitroxide probes modify the binding of other classes of peptides to lipid bilayers.

## ACKNOWLEDGMENT

We thank Dr. Vann Bennett for use of the CD equipment.

## REFERENCES

1. Deisenhofer, J., Epp, O., Miki, K., Huber, R., and Michel, H. (1985) *Nature 318*, 618−624.
2. Cowan, S. W., Schirmer, T., Rummel, G., Steiert, M., Ghosh, R., Pauptit, R. A., Jansonus, J. N., and Rosenbusch, J. P. (1992) *Nature 358*, 723−727.
3. Picot, D., Loll, P. J., and Garavito, R. M. (1994) *Nature 367*, 243−249.
4. Koepke, J., Hu, X., Menke, C., Schulten, K., and Michel, H. (1996) *Structure 4*, 581−597.
5. Valpuesta, J. M., Henderson, R., and Frey, T. G. (1990) *J. Mol. Biol. 214*, 237−251.
6. Henderson, R., Baldwin, J. M., Ceska, T. A., Zemlin, F., Beckman, E., and Downing, K. H. (1990) *J. Mol. Biol 213*, 899−929.
7. Havelka, W. A., Henderson, R., and Oesterhelt, D. (1995) *J. Mol. Biol. 247*, 726−738.
8. Unwin, N. (1998) *J. Struct. Biol. 121*, 181−190.
9. White, S. H. (1994) *Membrane Protein Structure. Experimental Approaches*, Oxford University Press, New York.
10. Nicholson, L. K., and Cross, T. A. (1989) *Biochemistry 28*, 9379−9385.
11. Jayasinghe, S., Barranger-Mathys, M., Ellena, J. F., Franklin, C., and Cafiso, D. S. (1998) *Biophys. J. 74*, 3023−3030.
12. Barranger-Mathys, M., and Cafiso, D. S. (1996) *Biochemistry 35*, 498−505.
13. Qin, Z., and Cafiso, D. S. (1996) *Biochemistry 35*, 2917−2925.
14. Weaver, A. J., Kemple, M. D., Brauner, J. W., Mendelsohn, R., and Prendergast, F. G. (1992) *Biochemistry 31*, 1301−1313.
15. Tamm, L. (1994) Physical studies of peptide-bilayer interactions, in *Membrane Protein Structure: Experimental Approaches* (White, S. H., Ed.) pp 283−313, Oxford University Press, New York.
16. Haris, P. I., and Chapman, D. (1995) *Biopolymers 37*, 251−263.
17. Rodionova, N. A., Tatulian, S. A., Surrey, T., Jahnig, F., and Tamm, L. K. (1995) *Biochemistry 34*, 1921−1929.
18. Abrams, F. S., and London, E. (1992) *Biochemistry 31*, 5312−5322.
19. Chattopadhyay, A., and London, E. (1987) *Biochemistry 26*, 39−45.
20. Kachel, K., Asuncion-Punzalan, E., and London, E. (1995) *Biochemistry 34*, 15475−15479.
21. Ren, J., Lew, S., Wang, Z., and London, E. (1997) *Biochemistry 36*, 10213−10220.
22. De Kroon, A. I. P. M., Soekarjo, M. W., De Gier, J., and De Kruijff, B. (1990) *Biochemistry 29*, 8229−8240.
23. Chung, L. A., Lear, J. D., and DeGrado, W. F. (1992) *Biochemistry 31*, 6608−6616.
24. Matsuzaki, K., Murase, O., Tokuda, H., Funakoshi, S., Fujii, N., and Miyajima, K. (1994) *Biochemistry 33*, 3342−3349.
25. Breukink, E., van Kraaij, C., van Dalen, A., Demel, R. A., Siezen, R. J., de Kruijff, B., and Kuipers, O. P. (1998) *Biochemistry 37*, 8153−8162.
26. McKnight, C. J., Briggs, M. S., and Gierasch, L. M. (1989) *J. Biol. Chem. 264*, 17293−17297.
27. Jones, J. D., and Gierasch, L. M. (1994) *Biophys. J. 67*, 1534−1545.
28. Jones, J. D., and Gierasch, L. M. (1994) *Biophys. J. 67*, 1546−1561.
29. Chupin, V., Killian, J. A., Breg, J., de Jongh, H. H. J., Boelens, R., Kaptein, R., and de Kruijff, B. (1995) *Biochemistry 34*, 11617−11624.
30. Keller, R. C. A., ten Berge, D., Nouwen, N., Snel, M. M. E., Tommassen, J., Marsh, D., and de Kruijff, B. (1996) *Biochemistry 35*, 3063−3071.
31. Voglino, L., McIntosh, T. J., and Simon, S. A. (1998) *Biochemistry 37*, 12241−12252.
32. McKnight, C. J., Rafalski, M., and Gierasch, L. M. (1991) *Biochemistry 30*, 6241−6246.
33. von Heinje, G. (1985) *J. Mol. Biol. 184*, 99−105.
34. Wickner, W., and Leonard, M. R. (1996) *J. Biol. Chem. 271*, 29514−29516.
35. Schatz, P., and Beckwith, J. (1990) *Annu. Rev. Genet. 24*, 215−248.
36. Joly, J. C., and Wickner, W. (1993) *EMBO J. 12*, 255−263.
37. Martoglio, B., Hofmann, M. W., Brunner, J., and Dobberstein, B. (1995) *Cell 81*, 207−214.
38. Batenburg, A. M., Brasseur, R., Russychaert, J.-M., van Scharrenburg, G. J., Slotbboom, A. J., Demel, R. A., and de Kruijff, B. (1988) *J. Biol. Chem. 263*, 4202−4207.
39. Rizo, J., Blanco, F. J., Kobe, B., Bruch, D., and Gierasch, L. M. (1993) *Biochemistry 32*, 4881−4894.
40. Wang, Z., Jones, J. D., Rizo, J., and Gierasch, L. M. (1993) *Biochemistry 32*, 13991−13999.
41. Ben-Tal, N., Honig, B., Peitzsch, R. M., Denisov, G., and McLaughlin, S. (1996) *Biophys. J. 71*, 561−575.
42. Epand, R. M., Stevenson, C., Bruins, R., Schram, V., and Glaser, M. (1998) *Biochemistry 37*, 12068−12073.

43. Denisov, G., Wanaski, S., Luan, P., Glaser, M., and McLaughlin, S. (1998) *Biophys. J. 74*, 731−744.
44. Ladokhin, A. S. (1999) *Biophys. J. 76*, 946−955.
45. New, R. R. C. (1990) *Liposomes, a Practical Approach*, IRL Press, New York.
46. Chen, P. S., Toribara, T. Y., and Warner, H. (1956) *Anal. Chem. 28*, 1756−1758.
47. McIntosh, T. J., and Holloway, P. W. (1987) *Biochemistry 26*, 1783−1788.
48. Sophianopoulos, J. A., Durham, S. J., Sophianopoulos, A. J., Ragsdale, H. L., and Cropper, W. P. (1978) *Arch. Biochem. Biophys. 187*, 132−137.
49. Ladokhin, A. S., Selsted, M. E., and White, S. H. (1997) *Biophys. J. 72*, 794−805.
50. MacDonald, R. C., Simon, S. A., and Baer, E. (1976) *Biochemistry 15*, 855−869.
51. Israelachvili, J. N. (1985) *Intermolecular and Surface Forces*, Academic Press, London.
52. White, S. H., and Wimley, W. C. (1994) *Curr. Opin. Struct. Biol. 4*, 79−86.

BI990099Q